Journal of the European Ceramic Society **17** (1997) 1049–1060

PII: S0955-2219(96)00248-8
0955-2219/97/$17.00

Microstructural Relations in BZS Pyrochlore-ZnO Mixtures

A. Mergen and W. E. Lee

University of Sheffield, Department of Engineering Materials, Sheffield, S1 3JD, UK

(Received 31 May 1996; revised version received 18 November 1996; accepted 25 November 1996)

Abstract

ZnO-pyrochlore mixtures were produced with different Bi_2O_3 and Sb_2O_3 contents but maintaining the Sb/Bi ratio = 1, which is the molar ratio in $Bi_{3/2}ZnSb_{3/2}O_7$ pyrochlore. Increased cooling rates and sintering temperatures reduced the amount of pyrochlore formed. Pyrochlore retards densification rates by retaining Bi_2O_3 and forming a skeletal network. Microstructures of quenched and slow-cooled samples were similar consisting of ZnO, spinel and a third phase. In the former this was Bi-rich intergranular phase(s) whereas it was pyrochlore in the latter. Although pyrochlore does not have a direct effect on the ZnO grain growth above 1050°C, it limits grain growth below this temperature. © *1997 Elsevier Science Limited.*

1 Introduction

The cubic pyrochlore structure[1] belongs to the space group Fd3m (No. 227) and has the general ideal formula of $A_2B_2X_6Z$ where A and B are cations and X and Z are anions.

A Bi_2O_3–ZnO–Sb_2O_3 pyrochlore phase is significant in microstructural evolution in ZnO varistor systems. Two chemical formulae have been proposed for this BZS pyrochlore. Wong[2] defined it as an oxygen-deficient pyrochlore with the formula $Bi_2(Zn_{4/3}Sb_{2/3})O_6$ while Inada[3,4] suggested its chemical composition was $Bi_{3/2}ZnSb_{3/2}O_7$. However, Kim *et al.*[5] produced the former composition and found three phases coexisting in the microstructure suggesting that it was not the correct pyrochlore formula. Ceramics produced using both stoichiometries and examined by X-ray diffraction (XRD), Scanning Electron Microscopy (SEM) and Transmission Electron Microscopy (TEM) confirmed the composition as $Bi_{3/2}ZnSb_{3/2}O_7$.[6,7]

Nonohmic zinc oxide (ZnO) ceramics are widely used as varistors for voltage stabilization or transient surge suppression in electronic circuits and electric power systems.[8] ZnO varistors are composed of ZnO grains, Bi_2O_3-containing grain boundaries responsible for the nonlinear response, and intergranular phases such as $Zn_7Sb_2O_{12}$ spinel and sometimes $Bi_{3/2}ZnSb_{3/2}O_7$ pyrochlore (BZS) whose formation strongly depends on the kind of additives used.[3,4] For example, if the α-spinel polymorph is stabilized by adding e.g. oxides of Cr, Co and Mn the amount of pyrochlore formed during slow cooling is minimized or eliminated. Since the phases formed in ZnO varistors consist mainly of the three oxides of ZnO–Bi_2O_3–Sb_2O_3 (ZBS), this ternary system plays a fundamentally important role in the microstructural formation, densification and grain growth.

Although this system has been studied extensively, the Sb/Bi ratio is generally kept below or above 1 because Sb/Bi = 1 corresponds to the pyrochlore composition so that at this ratio high levels of pyrochlore form in the microstructure. In the pure ZBS system BZS pyrochlore forms above 650°C and melts at 1280°C. Inada[4] found that the pyrochlore phase forms and disappears on heating, but in some cases is reproduced on slow cooling dependent on the kind of additive. This pyrochlore phase, if it forms, is the first to crystallize from the intergranular Bi_2O_3-rich liquid upon cooling from the sintering temperature.[9]

Although BZS pyrochlore plays no role in the nonohmic behaviour, since it is not a continuous intergranular layer,[4] it is undesirable in ZnO varistors because: (a) it retards densification because of a decreasing effect of the Bi-rich liquid phase on heating. Furthermore, on cooling, spinel and Bi_2O_3 react to form BZS pyrochlore which decreases the Bi_2O_3 level which is responsible for the nonlinear current voltage response of the grain boundaries, (b) it influences the growth of ZnO grains: reportedly pyrochlore has a restraining effect on ZnO grain growth at low temperatures,[10] (c) ZnO-pyrochlore interfaces do not show varistor behaviour[11] and (d) the breakdown field for bulk

ceramics decreases as the amount of pyrochlore in the microstructure is increased.[12]

Consequently, in the present work the ZnO–Bi_2O_3–Sb_2O_3 (ZBS) system was studied for different Bi_2O_3 and Sb_2O_3 contents but keeping the ratio of Sb/Bi always = 1 which corresponds to the atomic ratio in the pyrochlore, $Bi_{3/2}ZnSb_{3/2}O_7$, Bi:Zn:Sb = 3:2:3. Phase analysis of quenched and slow-cooled samples was made by XRD and the resulting microstructures investigated in the SEM and TEM. The densification behaviour and grain size were examined as a function of sintering temperature and additive content.

2 Experimental

ZnO–$Bi_{3/2}ZnSb_{3/2}O_7$ pyrochlore mixtures were made from powders prepared using conventional ceramic processing techniques. Three different mixtures were prepared:

I. 90 wt% ZnO and 10 wt% BZS pyrochlore
II. 85 wt% ZnO and 15 wt% BZS pyrochlore
III. 75 wt% ZnO and 25 wt% BZS pyrochlore

Hereafter these mixtures are designated as VP1, VP2 and VP3 respectively. The total weight% and mol% of each individual oxide for the three mixtures are given in Table 1. To prepare the mixtures, zinc oxide (ZnO, >99·9%), bismuth oxide (Bi_2O_3, >99·9%) and antimony oxide (Sb_2O_3, >99%) (Aldrich Chemical Company Ltd, Gillingham, Dorset, UK) were weighed according to the compositions given in Table 1 and wet-mixed in ethanol for 4 h using zirconia balls in a plastic container. After drying the resulting slurry at 130°C for 24 h, powders were calcined 4 h at 700°C to form pyrochlore and prevent the volatilization of Bi_2O_3 during sintering. After grinding the calcined powder in a mechanical agate mortar and pestle, it was uniaxially pressed at 150 MPa into pellets approximately 10 mm in diameter and 2 mm in thickness. These pellets were then heated in air at 300 K/h to a desired temperature between 900 and 1200°C and soaked for 1 h. Two different cooling cycles were followed after firing. Some samples were air-quenched from the firing temperature and others were cooled slowly at a rate of 300 K/h.

Table 1. Batch compositions of three different ZnO-pyrochlore mixtures with weight percentages of each oxide and their equivalent mol percentages

Mixture	*Fraction*	*ZnO*	*Bi_2O_3*	*Sb_2O_3*
VP1	wt%	91·25	5·38	3·37
	mol%	97·98	1·01	1·01
VP2	wt%	86·88	8·07	5·05
	mol%	96·85	1·57	1·57
VP3	wt%	78·13	13·45	8·42
	mol%	94·33	2·84	2·84

Heat treated pellets were analysed by XRD with a Philips diffractometer using Cu $K\alpha$ radiation from 10 to 85° 2θ at speed of 1°/min. XRD analyses of calcined powder and pellets, made from calcined powder heated to 900°C and quenched without holding, were performed to verify that only ZnO and pyrochlore exist before densification of the pellets started. The phases present in air-quenched and furnace-cooled samples were analysed by XRD of crushed sintered pellets. The relative amounts of spinel β-$Zn_7Sb_2O_{12}$, (I_{SP}), pyrochlore $Bi_{3/2}ZnSb_{3/2}O_7$, (I_{PS}) and bismuth oxide β-Bi_2O_3, (I_{BP}), were calculated using:

$$I_{SP} = \frac{I_S}{(I_S + I_P)}, \quad I_{PS} = \frac{I_P}{(I_P + I_S)}$$

$$\text{and } I_{BP} = \frac{I_B}{(I_B + I_P)} \qquad (1)$$

where I_S is the total peak height of (022), (311), (113) and (464) of β-$Zn_7Sb_2O_{12}$, I_p of (440) and (622) of $Bi_{3/2}ZnSb_{3/2}O_7$ and I_B of (221) and (402) of β-Bi_2O_3. The relative amounts of pyrochlore, spinel and bismuth oxide have previously been calculated using X-ray peak height ratios.[4,5,12,13]

The microstructures of the sintered pellets were investigated on thermally etched and unetched samples using SEM (Jeol 6400) and TEM (Jeol 200CX operated at 200 kV). Energy Dispersive Spectroscopy (EDS) was performed using LINK AN10000 and eXL systems on the SEM and TEM (Philips 420T, operated at 120 kV) respectively. The theoretical densities of the ZnO-pyrochlore mixtures were calculated using the rule of mixtures for the weight percentages of the starting oxides[14] and grain sizes of sintered air-quenched pellets were measured directly from photomicrographs of the etched samples by the linear intercept technique described by Mendelson.[15] Given the complex phase equilibria in these pellets the error in the density determinations may be large. Consequently, these measurements are used primarily for comparative purposes. Thermal etching was done for 10 min at ≈ 1050°C.

3 Results and Discussion

3.1 XRD of calcined powder

Although XRD analysis of calcined *loose powder* revealed some unreacted Bi_2O_3 in addition to pyrochlore, ZnO and Sb_2O_4 (Fig. 1(a)), no Bi_2O_3 was found and only ZnO and pyrochlore were observed in crushed *pellets* made from calcined

powder which had been quenched from 900°C without holding (Fig. 1(b)). This confirms that all the Bi_2O_3 and Sb_2O_3 formed pyrochlore before significant densification of the *pellets* occurred.

3.2 Effect of cooling rate on the formation of phases

XRD analysis of quenched pellets revealed that below 1000°C only ZnO and pyrochlore were present in all three mixtures so that the added Bi_2O_3 and Sb_2O_3 reacted with ZnO to form pyrochlore and no significant amounts of spinel or crystalline bismuth oxide were observed. However, traces of spinel (β) and bismuth oxide (β) were found at 1000°C which became more significant going from VP1 to VP3. In Figs 2(a) and (b) the amounts of spinel or bismuth oxide relative to the pyrochlore phase are plotted against sintering temperature. There is no significant transformation of pyrochlore until 1000°C but above 1000°C there is a sharp increase in the relative amounts of spinel and bismuth oxide as a result of reaction below.[4]

$$2\ Bi_3Zn_2Sb_3O_{14} + 17\ ZnO \xrightarrow{950\text{–}1050°C} 3\ Zn_7Sb_2O_{12}\ (\beta) + 3\ Bi_2O_3\ (\text{liquid}) \quad (2)$$

Above 1050°C only a trace of pyrochlore was observed while none was detected in samples quenched from 1200°C in all mixtures in agreement with Kim *et al.*[5] Figure 2 indicates that above 1050°C there is little change in the relative amounts of spinel and Bi_2O_3 compared to the increase between 1000 and 1050°C consistent with the transformation temperature of pyrochlore (950–1050°C).[4]

In slow-cooled samples of these mixtures sintered between 1050 and 1200°C XRD analysis reveals mainly ZnO and pyrochlore with traces of Bi_2O_3 and spinel. Figure 3 shows the relation between pyrochlore/spinel (Fig. 3(a)) and pyrochlore/bismuth oxide (Fig. 3(b)) peak ratio and sintering temperature. Generally, with increased sintering temperature, the amount of pyrochlore relative to the spinel or bismuth oxide decreases after cooling as observed by Olsson and Dunlop.[16] The re-formation of pyrochlore during slow cooling is due to the following reaction:[4]

$$3\ Zn_7Sb_2O_{12}\ (\beta) + 3\ Bi_2O_3\ (\text{liquid}) \xrightarrow{\text{slow cooling (960–850°C)}} 2\ Bi_3Zn_2Sb_3O_{14} + 17\ ZnO \quad (3)$$

It is suggested that the reason for the decrease in the amount of pyrochlore with increased sintering temperature is that at high temperatures spinel has undergone more grain growth which slows the reaction with Bi_2O_3-rich liquid so that less pyrochlore forms during slow cooling.[17]

As observed by others[4,12,18] these results reveal that cooling rate has a pronounced effect on the pyrochlore formation. Although quenched samples

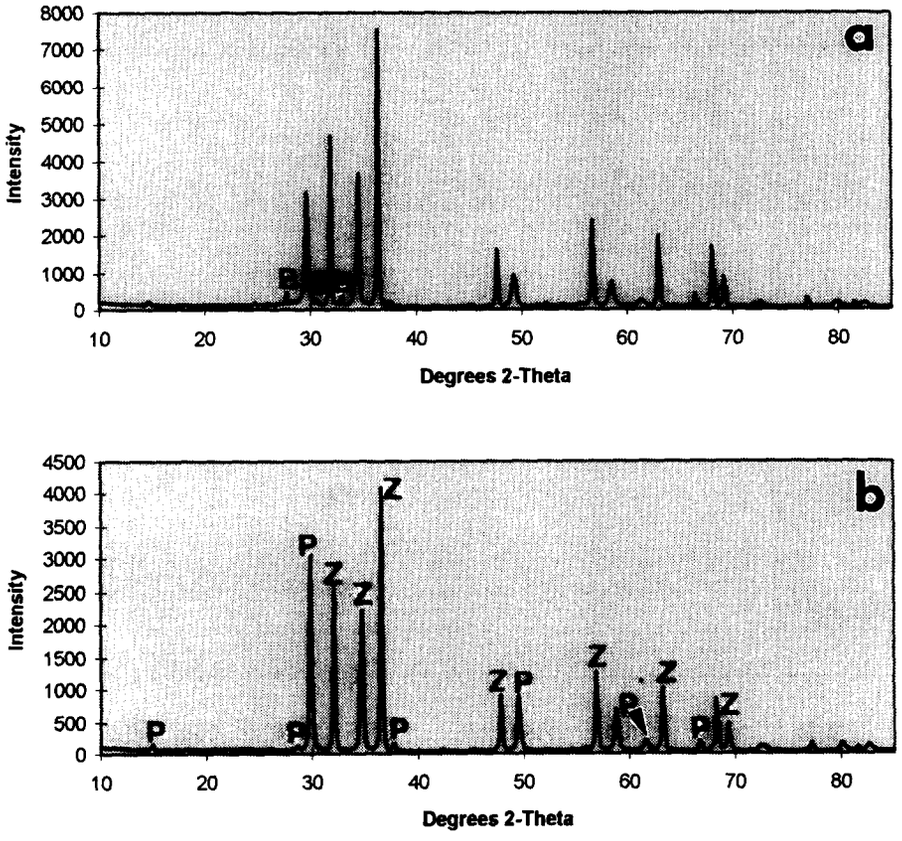

Fig. 1. XRD of (a) calcined *loose powder* of VP3 after 4 h at 700°C and (b) crushed *pellet* of VP3 made from calcined powder and quenched from 900°C without holding. P = $Bi_{3/2}ZnSb_{3/2}O_7$, Z = ZnO, B = Bi_2O_3 and S = Sb_2O_4.

were nearly free of pyrochlore above 1050°C, slow cooling led to formation of pyrochlore and as the sintering temperature increased the amount of pyrochlore decreased. This behaviour is thought to arise due to the slowing down of reaction (3) with increased cooling rate.

3.3 Densification behaviour of ZnO-pyrochlore mixtures

The relative percentage densities of samples quenched from different sintering temperatures are given in Fig. 4. There is no significant increase in density until 950°C. Density reached a maximum

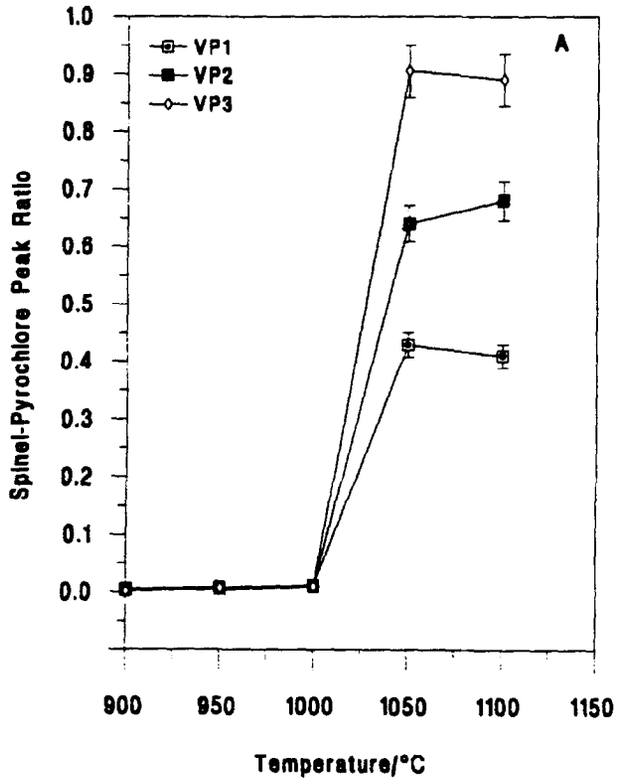

Fig. 2. Relative amount of (A) spinel and (B) bismuth oxide in quenched samples of VP1, VP2 and VP3 mixtures sintered at different temperatures for 1 h.

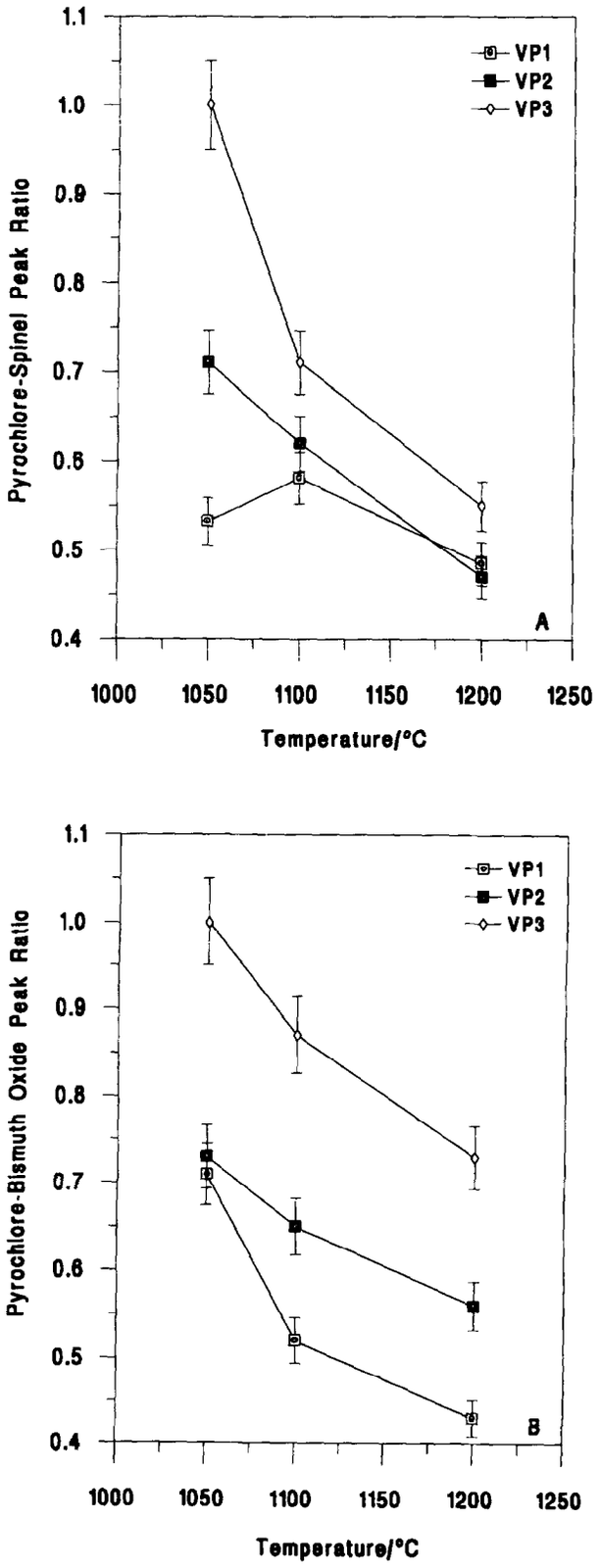

Fig. 3. Amount of pyrochlore relative to (A) spinel and (B) bismuth oxide in slow-cooled samples of VP1, VP2 and VP3 sintered for 1 h at different temperatures.

value at 1050°C and then decreased. The density increase above 950°C is most likely due to formation of Bi_2O_3 liquid (melting temperature of Bi_2O_3 = 825°C) from reaction of pyrochlore with ZnO (reaction (2)) although XRD analysis of quenched samples showed only a trace amount of crystalline Bi_2O_3 due to transformation of pyrochlore at 1000°C. In ZnO varistors densification occurs through a liquid phase which is formed by eutectic melting at around 750°C in the system $ZnO–Bi_2O_3$ for Sb/Bi <1[19,20] and through reaction of pyrochlore with ZnO between 950 and 1050°C for Sb/Bi ≥1.[4] Kim *et al.*[5] also observed similar densification behaviour in pellets with Sb/Bi = 1 i.e. a sharp increase after 950°C and then a maximum at around 1050°C. In the present work the ratio of Sb/Bi is 1 and all the available Bi_2O_3 was consumed to form pyrochlore below 950°C. Therefore densification started above 950°C instead of 750°C since there is no free Bi_2O_3 available to cause densification until this temperature. It can be concluded that pyrochlore retards densification of the mixtures by retaining Bi_2O_3.

At 1000°C the mixtures had notable density differences with density decreasing from VP1 to VP3. The reason for this can be explained using Fig. 5 which gives a measure of the phase content in each mixture quenched from 1000°C. The spinel and bismuth oxide contents were nearly constant for the three mixtures but there was a significant difference in the amount of pyrochlore.

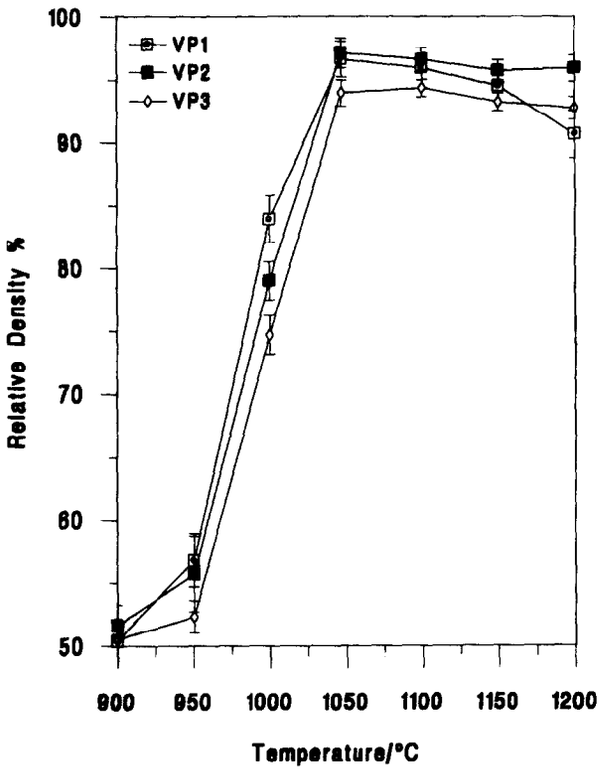

Fig. 4. Relative percentage densities of the quenched samples made from VP1, VP2 and VP3 after 1 h at different temperatures.

This suggests that pyrochlore plays an important role in determining the density of these mixtures at 1000°C and as the amount of pyrochlore increases, being maximum for VP3, the density of the mixture decreases, being minimum for VP3. Since pyrochlore (7·86 g/cm^3) has a higher density than ZnO (5·606 g/cm^3) and spinel (6·2 g/cm^3) the presence of pyrochlore might have been expected to lead to higher densities. The reason why density is low at 1000°C with high pyrochlore content is thought to be associated with the skeletal pyrochlore grain morphology as illustrated in Fig. 6. Densification is limited by the pyrochlore network in much the same way as the presence of a

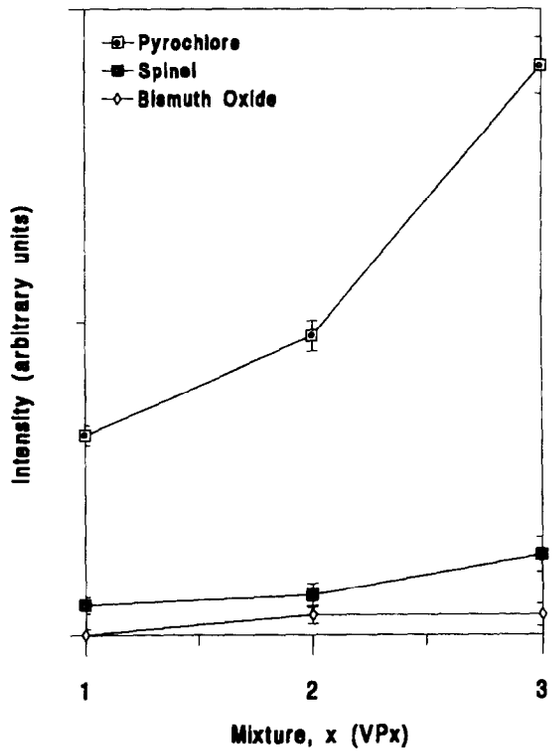

Fig. 5. Phase content in different mixtures quenched from 1000°C indicated by plotting the intensity of specific X-ray peaks for each phase. The total peak heights of (022), (311), (113) and (464) of spinel, (440) and (622) of pyrochlore and (221) and (402) of bismuth oxide were used for calculations.

Fig. 6. Backscattered electron SEM image of quenched sample made from VP2 and sintered at 1000°C for 1 h. Z = ZnO, P = Pyrochlore and Pr = Pore.

reinforcing phase inhibits densification in a ceramic matrix composite.

Above 1050°C the density of the three mixtures starts to decrease (Fig. 4) because of Bi_2O_3 evaporation.[21]

3.4 ZnO-pyrochlore mixture microstructures

3.4.1 Quenched samples

The microstructures of samples quenched from a sintering temperature of 1000°C consisted mainly of dark grey ZnO grains, white pyrochlore phase and dark pores (Fig. 6). However, XRD of this sample revealed traces of spinel and bismuth oxide so that it is expected that some of the dark grey/white phase is spinel/bismuth oxide. The microstructure was porous (~78% dense, Fig. 4) and ZnO grains were around 1 μm in size. The porosity was due to the pyrochlore phase which did not react enough to give sufficient Bi_2O_3 liquid for densification and grain growth by reaction (2). However, the microstructures of quenched samples (VP1, VP2 and VP3) sintered at temperatures of between 1050 and 1200°C consisted of ZnO grains, intergranular spinel and Bi_2O_3-rich phases and particles trapped within ZnO and spinel grains. A typical example of the phase distribution in samples quenched ≥ 1050°C is shown schematically in Fig. 7.

Figures 8(a) and (b) reveal the microstructure of quenched samples of VP2 and VP3 sintered 1 h at 1200°C with EDS analysis taken from each phase. Note the rounded morphology of the grains characteristic of the solution-precipitation stage of liquid phase sintering. Intragranular particles exist in both ZnO and spinel grains. In Figs 8(a) and (b) it can be clearly seen that some ZnO particles with a small amount of Bi_2O_3 were enveloped within spinel grains and some spinel particles, again with a small amount of Bi-rich phase, were trapped within ZnO grains. The spherical shape of these small intragranular particles suggests that they were trapped during grain growth.[22] Bi_2O_3-rich phase was distributed between ZnO and spinel grains. Spinel grains (submicron to 2 μm) were usually located in clusters and occasionally singly between ZnO grains (Fig. 9). In addition, some spinel particles with associated pores were also observed within ZnO grains (Fig. 9).

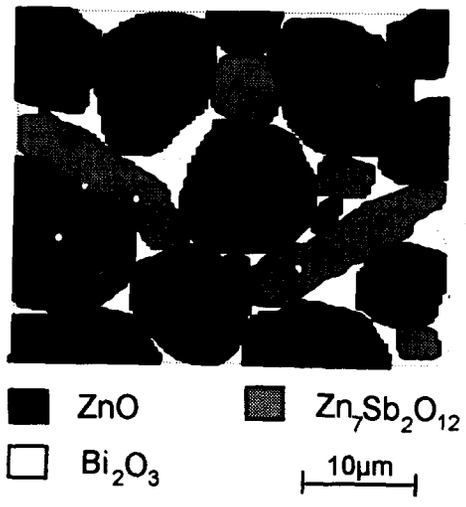

Fig. 7. Schematic representation of typical microstructure observed in quenched samples of VP1, VP2 and VP3 sintered 1 h at temperatures above 1050°C.

Microstructures of quenched samples (VP2 1100°C) were also examined in the TEM and revealed ZnO grains, spinel and Bi-rich phases. Bi-rich phases were observed at triple junctions and grain boundaries throughout the microstructure and were mostly crystalline. Electron diffraction and EDS analysis of such phases showed that they comprised Bi_2O_3 with Zn and Sb in solid solution. Inada[4,23] reported that Bi_2O_3 can dissolve a large amount of ZnO with a small amount of Sb_2O_3. Although XRD analysis of VP2 sintered 1 h at 1100°C indicated a trace of pyrochlore, none was observed in the region of microstructure examined in the TEM. However, an unknown phase was observed generally next to the Bi-rich phase and EDS analysis showed that it was rich in Zn, Sb and Bi. This phase may possibly be a pyrochlore which has a different stoichiometry from $Bi_{3/2}ZnSb_{3/2}O_7$.

3.4.2 Slow-cooled samples

Figure 10 is a schematic representation of the microstructure of a typical sample slow cooled from a sintering temperature of 1050–1200°C consisting mainly of ZnO with intergranular spinel and pyrochlore phases. Figures 11(a) and (b) are backscattered electron images of VP1 sintered at 1200 and 1050°C respectively with EDS of the pyrochlore while Fig. 12 is of VP3 sintered at 1200°C. These figures show black ZnO grains and grey/light spinel/pyrochlore phases with some intragranular particles within ZnO and spinel grains. The microstructures of slow-cooled samples were similar to those of quenched samples except they contained pyrochlore phase instead of Bi_2O_3.

TEM of these samples confirms these observations, e.g. Fig. 13 shows ZnO, pyrochlore and spinel phases in VP2 sintered 1 h at 1100°C. The pyrochlore has a similar morphology to the Bi-rich phase in quenched samples and, as observed in the SEM, it is distributed between ZnO grains and/or ZnO-spinel grains since it is formed from reaction of Bi-rich liquid phase with spinel during slow cooling. In addition, some Bi-rich crystalline

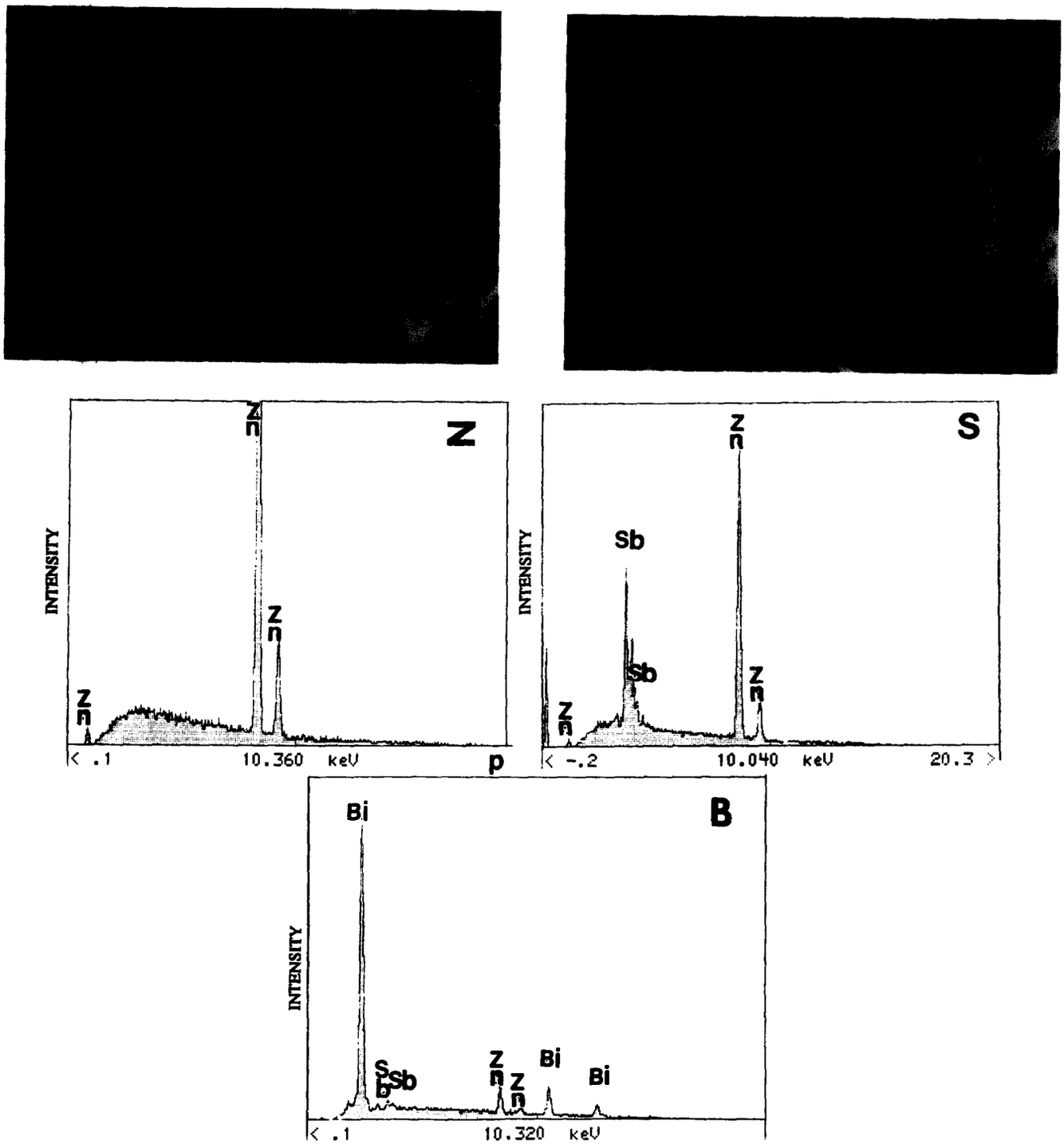

Fig. 8. SEM backscattered electron micrographs of unetched quenched samples of (A) VP2 and (B) VP3 sintered at 1200°C for 1 h indicating three different phases with EDS analysis and some intragranular particles. Z = ZnO, S = Spinel, B = Bi_2O_3.

phase was also observed generally at grain junctions in agreement with XRD of these samples which indicates crystalline Bi_2O_3.

3.5 ZnO grain size

Since ZnO grain size directly affects the electrical properties of ZnO varistors there have been a number of studies addressing sintering and grain growth. Kim *et al.*,[24] Senda and Bradt,[25] Dey and Bradt[26] and Hingorani *et al.*[27] examined the effect of Bi_2O_3 on the grain growth of ZnO and Kim *et al.*[22] and Senda and Bradt[28] investigated the ZnO grain size dependence on Sb_2O_3 content. In the present study the effect of different amounts of Bi_2O_3–Sb_2O_3 on the ZnO grain size (keeping the Sb_2O_3/Bi_2O_3 ratio always 1) has been examined for different additive contents. The mol% of each oxide (Bi_2O_3 and Sb_2O_3) was varied from 1·01 to 2·84 (Table 1).

The ZnO grain size in samples quenched from 1000°C was approximately 1 μm. Analysis of these samples by XRD and SEM (Fig. 6) revealed that these specimens contained considerably more pyrochlore than specimens sintered at and above

1050°C and this substantially decreased the volume fraction of Bi_2O_3 liquid phase at 1000°C. Two possible explanations for the small grain size at 1000°C are (a) lack of enough liquid phase since pyrochlore retains Bi_2O_3 and (b) pyrochlore particles might reduce grain boundary mobility since they form a skeletal structure of inclusion particles (Fig. 6). Kim *et al.*[24] and Senda and Bradt[25] obtained significant ZnO grain growth at 1000°C with excess Bi_2O_3. Another potential reason for the small ZnO grain size at 1000°C might simply be because at this temperature there is not enough atom mobility to cause grain growth. However, Senda and Bradt[25] measured grain growth of pure ZnO sintered 1 h at 900 and 1030°C and found grain sizes around 3 μm and 7 μm respectively indicating atom mobility is sufficient at these temperatures. In addition, Gupta and Coble[29] found a grain size of around 7 μm for the pure ZnO sintered 2 h at 1000°C.

Fig. 9. Backscattered electron image of a thermally etched VP1 sample sintered at 1050°C for 1 h indicating single spinel particles at grain boundaries and spherical pores and spinel particles within ZnO grains. Z = ZnO, S = Spinel and Pr = Pore.

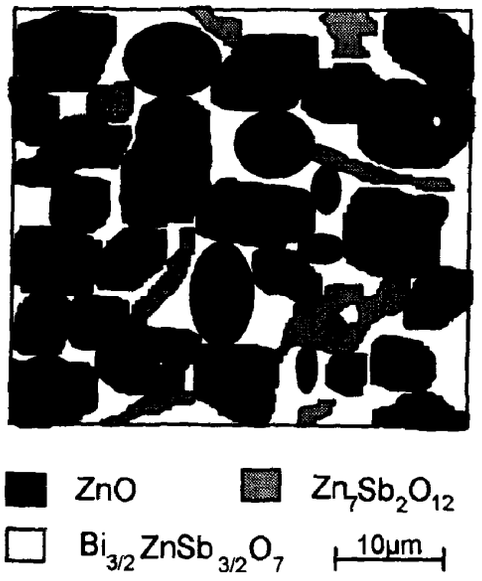

Fig. 10. Schematic representation of microstructure of slow-cooled samples from 1050, 1100 and 1200°C.

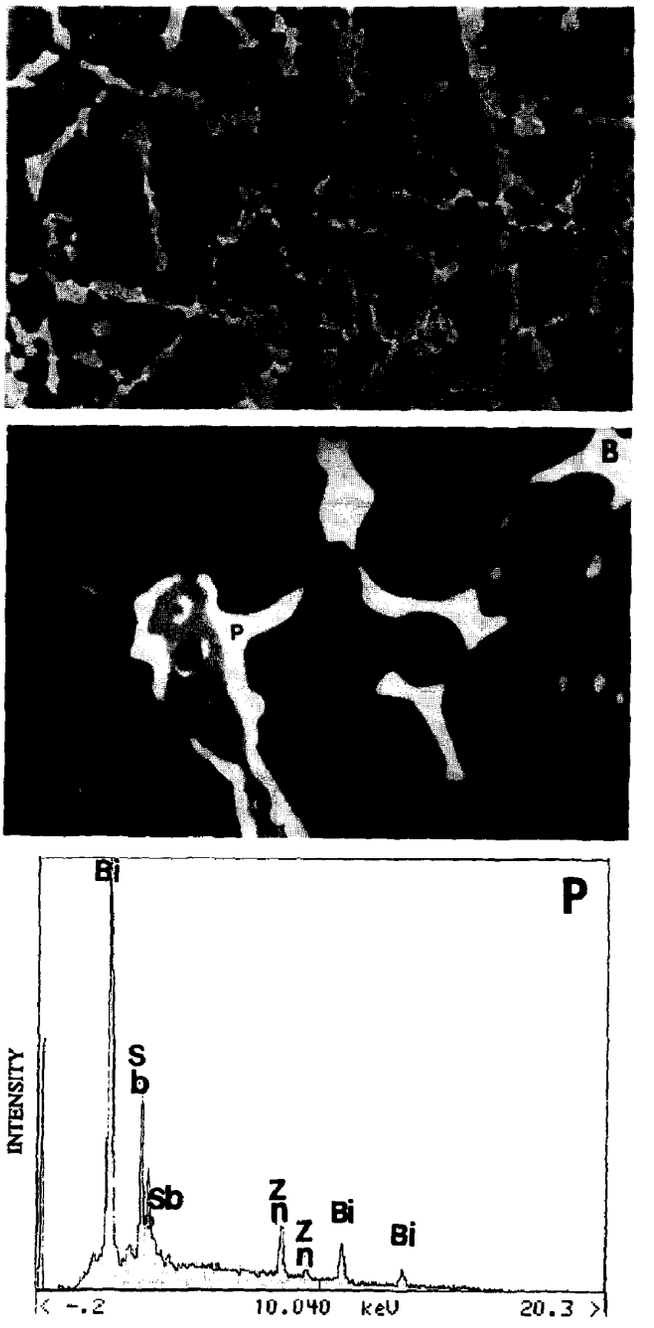

Fig. 11. Backscattered electron images of unetched slow-cooled VP1 sintered at (A) 1200°C and (B) 1050°C for 1 h showing the rod-like shape of spinel and indicating pyrochlore phase between the ZnO and ZnO-spinel grains with EDS analysis from pyrochlore. Z = ZnO, S = Spinel and P = Pyrochlore.

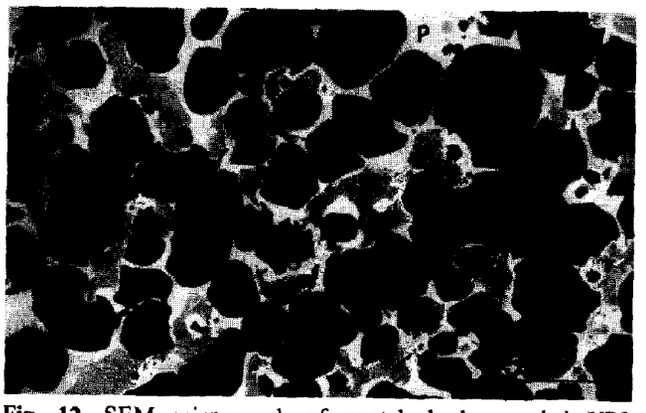

Fig. 12. SEM micrograph of unetched slow-cooled VP3 sintered 1 h at 1200°C revealing greater spinel content than Fig. 11. Z = ZnO, S = Spinel and P = Pyrochlore.

Figure 14 shows the microstructures of quenched samples of different mixtures sintered 1 h at 1100°C. All samples were thermally etched for grain size measurement since chemical etching in this system is difficult due to the high solubility of ZnO in acids and bases.[30,31] Although thermal etching may affect the grain growth of ZnO slightly, it is not believed to be significant.[31]

The ZnO grain size is plotted against sintering temperature (Fig. 15(a)) and mixture number

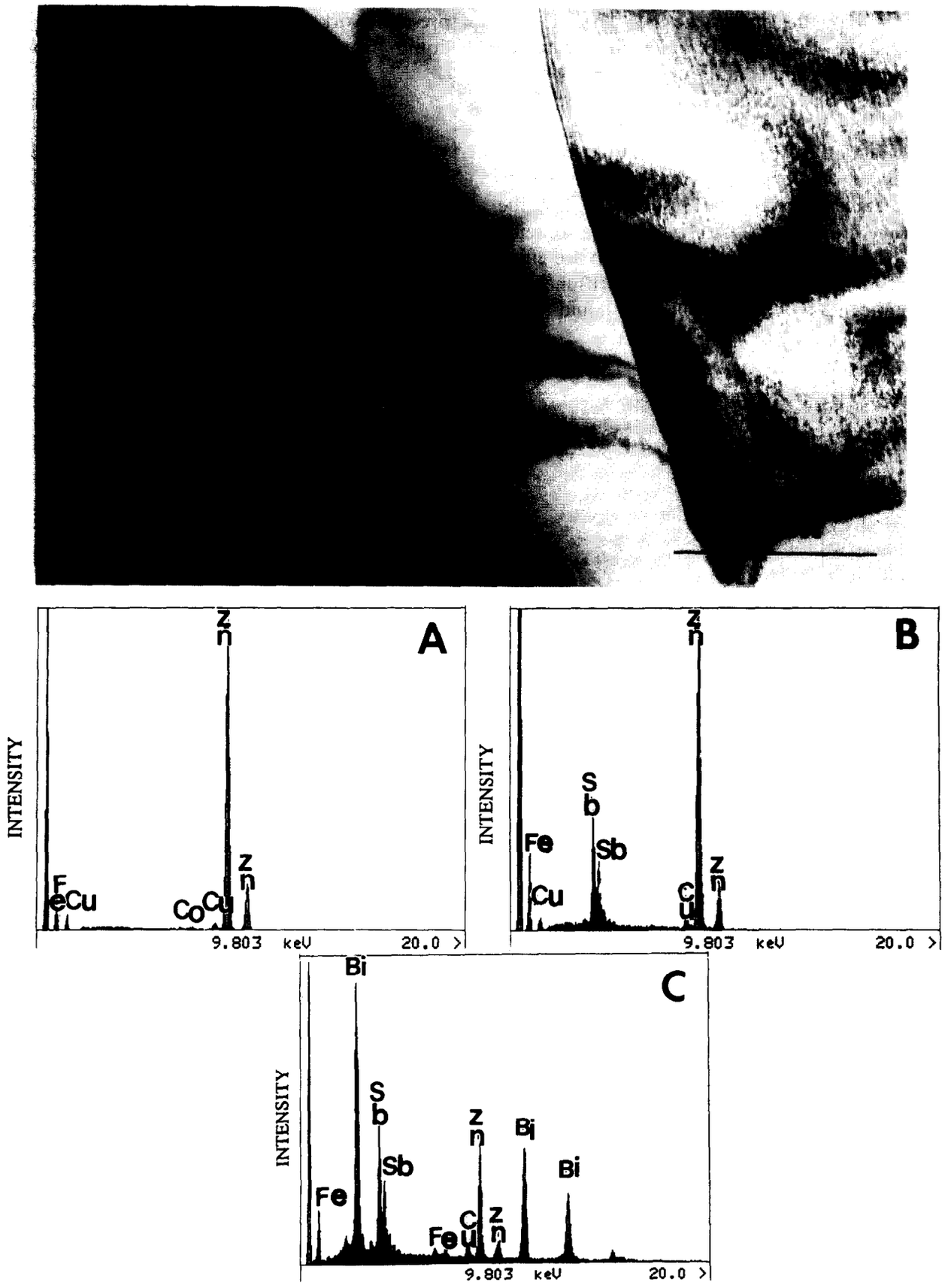

Fig. 13. TEM micrograph of slow-cooled VP2 sample sintered 1 h at 1100°C indicating intergranular pyrochlore phase between ZnO and spinel grains with EDS analysis from (A) ZnO (Z), (B) Spinel (S) and (C) Pyrochlore (P). Fe, Cu and Co peaps are artefacts

(Fig. 15(b)) in quenched samples and the average grain size is listed in Table 2. The average grain size consistently increases with sintering temperature and decreases from VP1 to VP3. The decrease in ZnO grain size with composition is related to the amount of liquid phase and spinel phase formed within the microstructure. Kim *et al.*[5] found that at 1200°C ZnO grain size decreases with increasing total additive content (0·75–3 mol% Bi_2O_3+Sb_2O_3) for Sb/Bi = 1 and they attributed this behaviour to the increase in the volume fraction of $Zn_7Sb_2O_{12}$ and liquid Bi_2O_3 in intergranular regions. In the present study, two mechanisms might be responsible for the decreased grain size with additive contents (Bi_2O_3+Sb_2O_3): (a) spinel particles which are effective by a particle drag mechanism and (b) increase in the thickness of the Bi_2O_3-rich liquid layer which increases the diffusion distance and lowers the rate of ZnO grain growth.

Kim *et al.*[22] and Senda and Bradt[28] reported that $Zn_7Sb_2O_{12}$ spinel causes grain growth inhibition in the ZnO–Sb_2O_3 system by a grain boundary particle drag mechanism. However, in the present work spinel formed along with Bi_2O_3 liquid from transformation of pyrochlore by

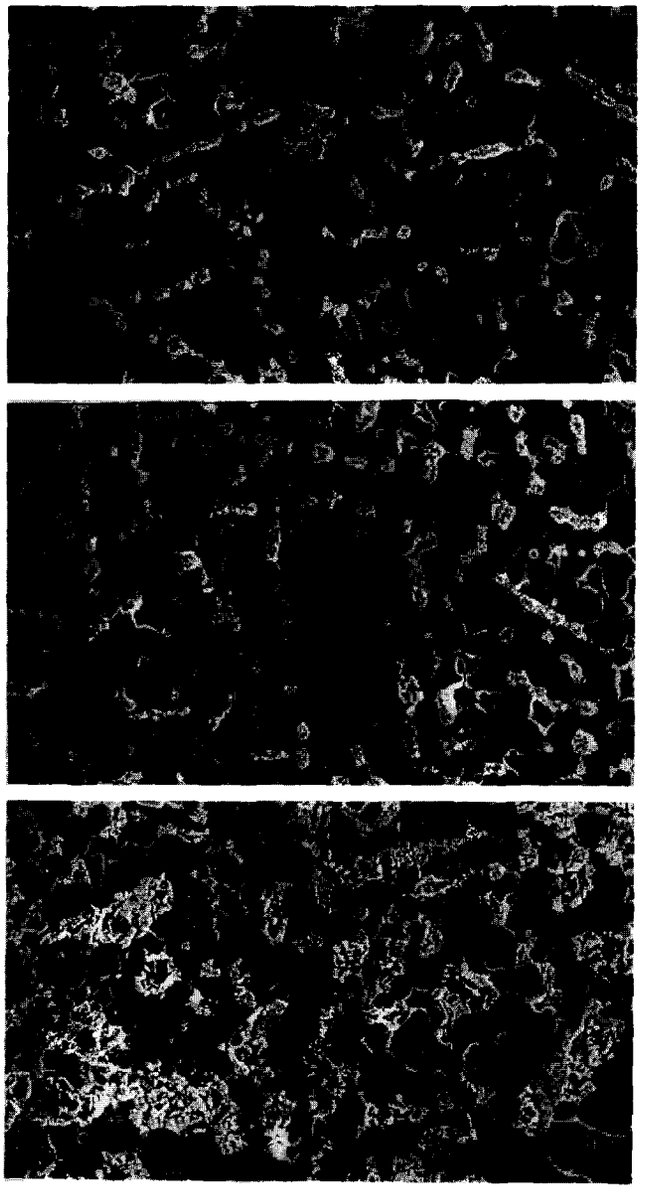

Fig. 14. SEM micrographs of quenched samples made from (A) VP1, (B) VP2 and (C) VP3 and sintered for 1 h at 1100°C.

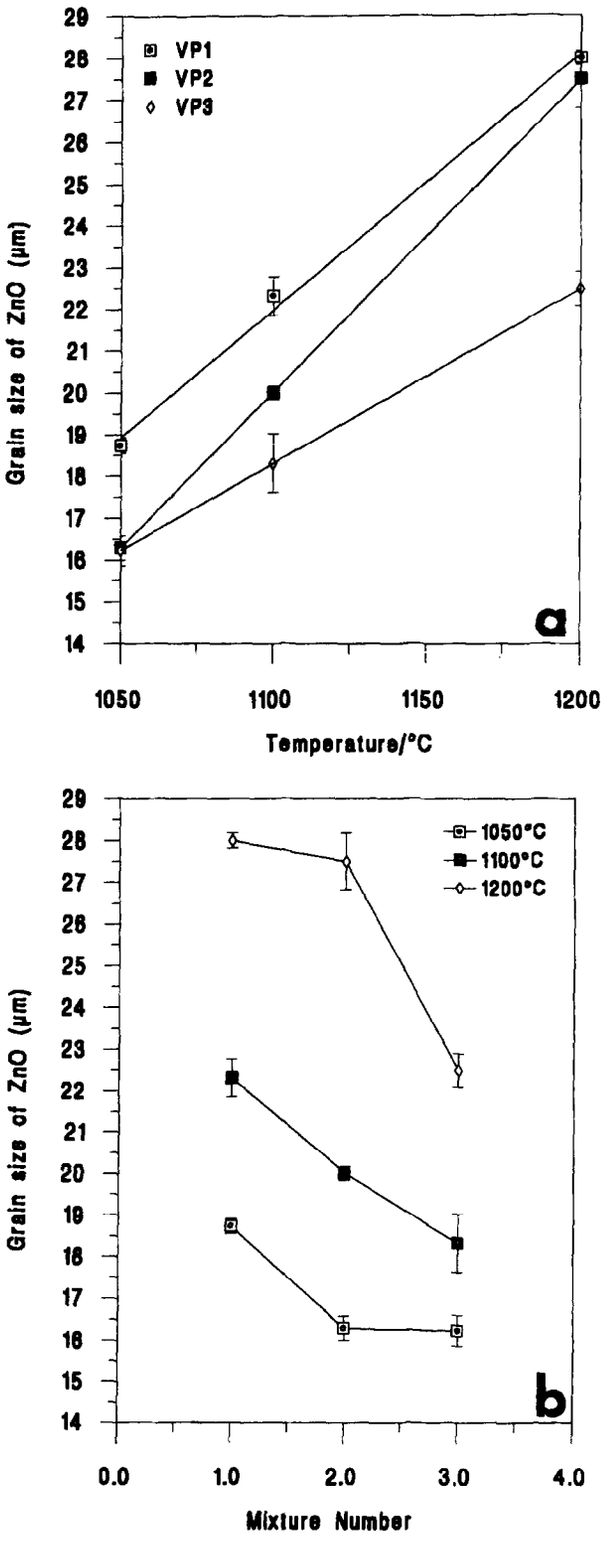

Fig. 15. Grain size of ZnO as a function of (a) sintering temperature and (b) total amount of additives (or mixture number) indicating that grain size increases with sintering temperature and decreases with total amount of additives.

Table 2. ZnO grain size in samples quenched from different sintering temperatures for different compositions

	Grain size (μm)		
Comp. / *T°C*	*VP1*	*VP2*	*VP3*
1050	18·73 ± 0·18	16·29 ± 0·29	16·22 ± 0·37
1100	22·31 ± 0·46	20·01 ± 0·16	18·32 ± 0·70
1200	28·00 ± 0·17	27·50 ± 0·67	22·49 ± 0·40

reaction (2). The liquid always exists during sintering which prevents ZnO grains being pinned by spinel particles so this is not a valid mechanism for the grain size decrease in this work. Senda and Bradt[25] investigated the effect of Bi_2O_3 content between limits of 0·09 and 0·72 mol% on the grain growth of ZnO and reported that ZnO grain size increases with Bi_2O_3 content. However, Dey and Bradt[26] examined the effect of higher Bi_2O_3 contents, 0·54–2·33 mol%, on the ZnO grain growth and found that ZnO grain size decreases with increasing Bi_2O_3. They concluded that during the liquid phase sintering of ZnO in the presence of Bi_2O_3 the rate-controlling mechanism of ZnO grain growth changes from one of phase boundary reaction at low levels of Bi_2O_3 to one of diffusion through the liquid phase at higher Bi_2O_3 contents. In the present work, the mol% of Bi_2O_3 changes from 1·01 to 2·84 and it is observed that with increasing Bi_2O_3 content ZnO grain size decreases and it is thought that the same mechanism suggested by Dey and Bradt[26] might also be effective for the decrease in ZnO grain size here. If Zn and O diffusion through the Bi_2O_3-rich liquid controls the ZnO grain growth, then ZnO grain growth rate is inversely proportional to the thickness of the layer between the ZnO grains. In other words, as the Bi_2O_3 mol% increases the amount of liquid increases and the greater material transport path decreases the grain growth rate.

In addition, the pyrochlore phase does not directly affect the ZnO grain size above 1050°C since it mostly transforms to spinel and Bi_2O_3-rich liquid. However, pyrochlore has a restraining effect on the grain growth of ZnO at low temperatures as suggested by Gupta[10] because (a) it retains Bi_2O_3 and (b) pyrochlore particles in a skeletal network might reduce grain boundary mobility. Table 2 and Fig. 15(b) indicate that higher pyrochlore contents in the mixtures at low temperatures led to smaller ZnO grain size after sintering above 1050°C since higher pyrochlore content results in formation of more Bi_2O_3-rich liquid during sintering. Consequently, pyrochlore indirectly affects the ZnO grain size at high temperatures (>1050°C).

4 Conclusions

(1) Phase analysis of quenched and slow-cooled samples revealed that cooling rate and sintering temperature have a pronounced effect on pyrochlore formation. Increasing cooling rates and sintering temperatures resulted in less pyrochlore in the microstructure.

(2) Pyrochlore retards densification of the mixtures by retaining Bi_2O_3 and by forming a skeletal network in much the same way as reinforcing fibres inhibit densification of a ceramic matrix composite.

(3) The microstructures of quenched and slow-cooled samples were similar except for the phase present in addition to the ZnO and spinel. In quenched samples this comprised Bi-rich phases whereas in slow-cooled samples it was pyrochlore.

(4) ZnO grain growth decreases with total amount of additives (Bi_2O_3+Sb_2O_3 = 2·02–5·68 mol%) and the likely mechanism responsible for this is an increase in the thickness of the Bi-rich intergranular layer so that the diffusion distance for Zn and O through the liquid is increased.

(5) Pyrochlore has a restraining effect on ZnO grain size at low temperatures (<1050°C) because (a) it retains Bi_2O_3-rich liquid and (b) pyrochlore particles might reduce grain boundary mobility. However, pyrochlore does not have a direct effect on the ZnO grain growth above 1050°C since it decomposes to spinel and Bi_2O_3.

Acknowledgement

This work was sponsored by the Turkish Ministry of Education in the form of a scholarship (A.M.).

References

1. Subramanian, M. A., Aravamudan, G. and Subba Rao, G. V., Oxide pyrochlores—a review. *Prog. Sol. State Chem.*, 1983, **15**, 55–143.
2. Wong, J., Microstructural and phase transformation in a highly non-ohmic metal oxide varistor ceramic. *J. Appl. Phys.*, 1975, **46**(4), 1653–1659.
3. Inada, M., Crystal phases of nonohmic zinc oxide ceramics. *Jap. J. Appl. Phys.*, 1978, **17**(1), 1–10.
4. Inada, M., Formation mechanism of nonohmic zinc oxide ceramics. *Jap. J. Appl. Phys.*, 1980, **19**(3), 409–419.
5. Kim, J., Kimura, T. and Yamaguchi, T., Sintering of zinc oxide doped with antimony oxide and bismuth oxide. *J. Am. Ceram. Soc.*, 1989, **72**(8), 1390–1395.
6. Mergen, A., Electrical ceramics with the pyrochlore crystal structure in the ZnO–Bi_2O_3–Sb_2O_3 and PbO–MgO–Nb_2O_5 systems. Ph.D. Thesis, University of Sheffield, UK, 1996.

7. Mergen, A. and Lee, W. E., Fabrication and crystal chemistry of $Bi_{3/2}ZnSb_{3/2}O_7$ pyrochlore. *J. Euro. Ceram. Soc.*, 1996, **16**, 1041–1050.
8. Matsuoka, M., Progress in research and development of zinc oxide varistors. In *Advances in Ceramics, Grain Boundary Phenomena in Electronic Ceramics*, ed. L. M. Levinson and D. C. Hill. Am. Ceram. Soc. Inc., 1981, pp. 290–308.
9. Olsson, E., Falk, L. K. L., Dunlop, G. L. and Osterlund, R., The microstructure of a ZnO varistor material. *J. Mater. Sci.*, 1985, **20**, 4091–4098.
10. Gupta, T. K., Application of zinc oxide varistors. *J. Am. Ceram. Soc.*, 1990, **73**(7), 1817–1840.
11. Olsson, E. and Dunlop, G. L., Characterisation of individual interfacial barriers in a ZnO varistor material. *J. Appl. Phys.*, 1989, **66**(8), 3666–3675.
12. Olsson, E. and Dunlop, G. L., Development of intergranular microstructure in ZnO varistor materials. *Proceedings of the 6th CIMTEC, High Tech Ceramics*, ed. P. Vincenzini. Elsevier Science BV, Amsterdam, 1987, pp. 1765–1774.
13. Kim, J. C. and Goo, E., Morphology and formation mechanism of the pyrochlore phase in ZnO varistor materials. *J. Mater. Sci.*, 1989, **24**, 76–82.
14. Lee, W. E. and Rainforth, W. M., *Ceramic Microstructures, Property Control by Processing.* Chapman and Hall, London, 1994, p. 69.
15. Mendelson, M. I., Average grain size in polycrystalline ceramics. *J. Am. Ceram. Soc.*, 1969, **52**(8), 443–446.
16. Olsson, E. and Dunlop, G. L., The effect of Bi_2O_3 content on the microstructure and electrical properties of ZnO varistor materials. *J. Appl. Phys.*, 1989, **66**(9), 4317–4324.
17. Inada, M. and Matsuoka, M., Formation mechanism of nonohmic ZnO Ceramics. In *Advances in Ceramics. Vol. 7, Additives and Interfaces in Electronic Ceramics*, ed. M. F. Yan and A. H. Heuer. The Am. Ceram. Soc., Ohio, 1983, pp. 91–105.
18. Olsson, E., Dunlop, G. and Osterlund, R., Development of functional microstructure during sintering of a ZnO varistor material. *J. Am. Ceram. Soc.*, 1993, **76**(1), 65–71.
19. Wong, J. and Morris, W. G., Microstructure and phases in nonohmic $ZnO–Bi_2O_3$ ceramics. *Am. Ceram. Soc. Bull.*, 1974, **53**(11), 816–820.
20. Hwang, J. H., Mason, T. O. and Dravid, V. P., Microanalytical determination of ZnO solidus and liquidus boundaries in the $ZnO–Bi_2O_3$ system. *J. Am. Ceram. Soc.*, 1994, **77**(6), 1499–1504.
21. Asokan, T., Iyengar, G. N. K. and Nagabhushana, G. R., Studies on microstructure and density of sintered ZnO-based non-linear resistors. *J. Mater. Sci.*, 1987, **22**, 2229–2236.
22. Kim, J., Kimura, T. and Yamaguchi, T., Microstructure development in Sb_2O_3-doped ZnO. *J. Mater. Sci.*, 1989, **24**, 2581–2586.
23. Inada, M., Effects of heat-treatment on crystal phases, microstructure and electrical properties of nonohomic zinc oxide ceramics. *Jap. J. Appl. Phys.*, 1979, **18**(8), 1439–1446.
24. Kim, J., Kimura, T. and Yamaguchi, T., Effect of bismuth oxide content on the sintering of zinc oxide. *J. Am. Ceram. Soc.*, 1989, **72**(8), 1541–1544.
25. Senda, T. and Bradt, R. C., Grain growth in sintered ZnO and $ZnO–Bi_2O_3$ ceramics. *J. Am. Ceram. Soc.*, 1990, **73**(1), 106–114.
26. Dey, D. and Bradt, R. C., Grain growth of ZnO during Bi_2O_3 liquid-phase sintering. *J. Am. Ceram. Soc.*, 1992, **75**(9), 2529–2534.
27. Hingorani, S., Shah, D. O. and Multani, M. S., Effect of process variables on the grain growth and microstructure of $ZnO–Bi_2O_3$ varistors and their nanosize ZnO precursors. *J. Mater. Res.*, 1995, **10**(2), 461–467.
28. Senda, T. and Bradt, R. C., Grain growth of zinc oxide during the sintering of zinc oxide–antimony oxide ceramics. *J. Am. Ceram. Soc.*, 1991, **74**(6), 1296–1302.
29. Gupta, T. K. and Coble, R. L., Sintering of ZnO: I, Densification and grain growth. *J. Am. Ceram. Soc.*, 1968, **51**(9), 521–525.
30. Lide, D. R., *Handbook of Chemistry and Physics*, 73rd edn. Boca Raton, FL, 1992–1993.
31. Karakas, Y., Chemical processing, phase evolution, grain growth and electrical properties in ZnO varistor prepared by oxide coprecipation process. Ph.D. Thesis, University of Sheffield, UK, 1995.